

Coulomb gap in a model with finite charge transfer energy.

S. A. Basylko¹, P. J. Kundrotas^{2,3}, V. A. Onischouk^{1,2}, E. E. Tornau^{2,4} and A. Rosengren²

¹Joint Institute of Chemical Physics of Russian Academy of Sciences, 117 977 Kosygin Str. 4, Moscow, Russia

²Department of Physics/Theoretical physics, Royal Institute of Technology, SE-100 44 Stockholm, Sweden

³Faculty of Physics, Vilnius University, Sauletekio al. 9, LT-2040, Vilnius, Lithuania

⁴Semiconductor Physics Institute, Goštauto 11, LT-2600 Vilnius, Lithuania

(Received

)

The Coulomb gap in a donor-acceptor model with finite charge transfer energy Δ describing the electronic system on the dielectric side of the metal-insulator transition is investigated by means of computer simulations on two- and three-dimensional finite samples with a random distribution of equal amounts of donor and acceptor sites. Rigorous relations reflecting the symmetry of the model presented with respect to the exchange of donors and acceptors are derived. In the immediate neighborhood of the Fermi energy μ the density of one-electron excitations $g(\varepsilon)$ is determined solely by finite size effects and $g(\varepsilon)$ further away from μ is described by an asymmetric power law with a non-universal exponent, depending on the parameter Δ .

PACS numbers: 71.23.-k, 71.30.+h, 71.45.Gm

I. INTRODUCTION

Doping of solids might lead to drastic qualitative changes in their properties. The metal-insulator transition (MIT) is a spectacular manifestation of this. The understanding of the driving forces of the MIT is a long-standing problem. In the early seventies, the prediction¹ was made that on the dielectric side of the MIT the long-range Coulomb interactions deplete the density of one-electron excitations (DOE) $g(\varepsilon)$ near the Fermi energy μ . Further, analytical calculations of $g(\varepsilon)$ with Coulomb correlation taken into consideration have been performed on the metallic side of the MIT. Altshuler and Aronov² showed that for the metallic case $g(\varepsilon)$ in three dimensions has a cusp-like dependence $g(\varepsilon) \sim |\varepsilon - \mu|^{1/2}$ near μ . This was later confirmed in electron tunneling experiments for amorphous alloys³ and granular metals⁴.

On the insulating side of the MIT charge transport occurs via inelastic electron tunneling hopping between states localized on the impurity sites with one-electron energies close to μ . Mott⁵ demonstrated that at low temperatures electrons seek accessible energy states by hopping distances beyond the localization length, leading to a hopping conductivity $\sigma(T) \sim \exp(-T_0/T)^\nu$ with T_0 being a characteristic temperature depending on localization length and with the hopping exponent $\nu = 1/4$ for the non-interacting case in three dimensions. Efros and Shklovskii⁶ (ES) argued that the ground state of a system with long-range Coulomb interactions is stable with respect to one-particle excitations only if $g(\varepsilon)$ in the vicinity of μ has the symmetric shape

$$g(\varepsilon) \sim |\varepsilon - \mu|^{D-1} \quad (1)$$

with the universal exponent $D - 1$ depending only on the dimensionality D of the system. In particular, ES predicted that in $D = 3$ $g(\varepsilon) = \frac{3}{\pi} \left(\frac{\chi}{e^2}\right)^3 (\varepsilon - \mu)^2$, where χ is the dielectric constant and e is the electron charge.

Because $g(\varepsilon)$ vanishes only at $\varepsilon = \mu$, this is called a “soft” Coulomb correlation gap with a width $\Delta\varepsilon \sim e^3(N_0/\chi^3)^{1/2}$, where N_0 is the DOE far away from μ . The power law (1) gives⁷ a hopping exponent $\nu = D/(D + 3)$ at low temperatures, so for three-dimensional system with long-range Coulomb interactions $\nu = 1/2$.

The intriguing hypothesis about universality of (1) has stimulated further theoretical research, both analytical⁸ and numerical^{9–13}. To establish the hypothesis (1) Efros¹⁴ used the ground-state stability conditions for localized electrons (LES) with respect to charge transfer

$$\varepsilon_j - \varepsilon_i - \frac{e^2}{\chi r_{ij}} > 0, \quad (2)$$

where ε_i and ε_j are the one-particle energies of a neutral donor on a site i and of a charged donor on a site j , respectively, and r_{ij} is the distance between the sites i and j . The conditions (2) were used to heuristically derive a non-linear integral equation for $g(\varepsilon)$ ^{14–17} and then asymptotic analysis of this equation leads¹⁴ to the power law (1).

LES have been studied using the so-called classical donor-acceptor ($d-a$) model (see, e. g. Ref. 15). Within this model, the system considered is modeled by a continuous sample with randomly distributed $k \times N$ ($k \leq 1$) acceptor and N donor sites. Each acceptor site is negatively charged whereas out of N only $k \times N$ donors have a positive charge which leads to a large number of configurations of charged donors. Moreover, each of these configurations must obey not only conditions (2) but also more complicated conditions related to many-particles excitations (e. g., charge transfer involving four, six, etc. sites). Efros conjecture about the *universality* implies that $g(\varepsilon)$ does not depend on peculiarities of the particular model and, as a consequence, further theoretical studies of LES^{9,11–13} were confined to a *lattice d-a* model proposed in Ref. 14. In this model, N donors are

localized on all the sites of a D -dimensional lattice and the negative charge from $k \times N$ acceptors is uniformly smeared over the lattice sites so that each site i has a charge $e(n_i - k)$, where $n_i = 1$ if a donor on the site i is ionized and $n_i = 0$ if a donor is neutral. Disorder in this model is ensured by introducing randomly distributed one-site potentials. Monte Carlo simulations¹² on very large specimens of the lattice d - a model, however, have given rise to doubts about the universality of the $g(\varepsilon)$ behavior.

Another hint about possible non-universal behavior of $g(\varepsilon)$ has come from the intriguing and still not completely unfolded problem whether the so called spin-glass phase does exist in the classical d - a model (see, e. g. Ref. 18–20). Grannan and Yu¹⁸ studied the classical three-dimensional d - a model with $k = 0.5$ but with the total acceptor charge uniformly distributed over donor sites as in the lattice d - a model. In this case, the classical d - a model is equivalent to a model of Ising spins, localized on randomly distributed sites, with pairwise Coulomb interactions, a model in which a transition into the spin-glass state was found¹⁸ to occur at non-zero temperature. It was then concluded that such a transition should exist in *all* d - a models (with and without smearing of negative charge, defined on a lattice or on a continuous sample) as well because of the Efros universality hypothesis. Voita and Schreiber²⁰, however, have shown that the spin glass transition does not exist in the lattice $d - a$ model¹⁴. Besides, in recent work by one of us¹⁹ it was unequivocally demonstrated that the ground state of the classical d - a model and that of the model studied in Ref. 18 are qualitatively different. An analysis of histograms $\mathcal{H}[Q_{\alpha\beta}]$ of the so called overlaps $Q_{\alpha\beta} = \frac{1}{N} \sum_i \delta(n_i^\alpha, n_i^\beta)$ (here α and β refer to different pseudo-ground states (PGS) obtained by direct descents) has revealed that, indeed, for the model studied in Ref. 18 $\mathcal{H}[Q_{\alpha\beta}]$ has a symmetric Gaussian shape with the maximum at $\langle Q_{\alpha\beta} \rangle = 0$ and with the dispersion $\langle Q_{\alpha\beta}^2 \rangle \sim N^{-1}$. This means that a large number of microscopically different PGS's does exist in the model and according to Parisi's theory²¹ this implies the existence of a spin-glass state at low temperatures. Further Monte Carlo simulations at finite temperatures¹⁹ revealed the typical finite-size scaling of the spin-glass susceptibility. In the classical d - a model, however, $\mathcal{H}[Q_{\alpha\beta}]$ has its maxima at $\langle Q_{\alpha\beta} \rangle = 1$ which means that all PGS's generated are the same from microscopical point of view. The absence of microscopically different PGS's in the classical d - a model was explained¹⁹ by the pinning of all PGS's on the electric field created by the discretely distributed acceptor charges.

Therefore, it is highly desirable to study the properties of not only the classical d - a model, but of its various modifications as well. In the present work we consider a modified classical d - a model (MCDAM) in which acceptors can be neutral, so the energy Δ of the charge transfer from a donor to an acceptor ($d^0 + a^0 \rightarrow d^+ + a^-$, where d^0 , d^+ , a^0 , a^- stand for a neutral donor, a charged donor, a

neutral acceptor, a charged acceptor, respectively) has to be finite. The classical d - a model might be then viewed as the limit of the MCDAM as $\Delta \rightarrow \infty$. We have investigated the shape of the Coulomb gap (i. e. $g(\varepsilon)$ both for donor and acceptors in the vicinity of the Fermi level) in two- and three-dimensional MCDAMs at $T=0$ and found that the behavior of $g(\varepsilon)$ is in strong contradiction to the Efros conjecture about the universality of $g(\varepsilon)$. The rest of the paper is organized as follows. In Section II we introduce the MCDAM and arrive at some rigorous results which follow from a symmetry of the MCDAM with respect to the exchange of donor and acceptor sites. Further, the algorithm of energy minimization for the MCDAM including a discussion about inherent finite size effects is presented in Section III. Section IV is devoted to a description of the main results obtained. In Section V we discuss possible causes of universality violation in the MCDAM, analyze experimental data available in the literature and predict possible experimental situations in which the non-universal behavior of $g(\varepsilon)$ might be observed. And finally, a summary is presented in Section VI.

II. BACKGROUND

A. Model

We consider a D -dimensional system of volume L^D , in which an equal number of acceptor and donor sites N are allocated according to the Poisson distribution with a density $n = N \times L^{-D}$. It is convenient to choose energy unit E_0 as an energy of the Coulomb interaction between a pair of acceptors, say, localized on the average distance $n^{-1/D}$, $E_0 = e^2 n^{1/D} / \chi$. In typical bulk semiconductors $n \sim 10^{18} \text{ cm}^{-3}$ and $\chi \sim 10$, so $E_0 \sim 0.02 \text{ eV}$. Hereafter all expressions will be written in dimensionless units $n^{-1/D}$ for length and E_0 for energies. A microscopic state of a particular spatial arrangement of the donor and acceptor sites (henceforth referred to as the sample \mathbf{R}) is determined by a set of occupation numbers $(n_a, n_d) \equiv \{n_a(i), n_d(k), i = 1, 2, \dots, N, k = 1, 2, \dots, N\}$ determined in the following way. For the acceptors, $n_a(i) = 1$ if an acceptor on an acceptor site i has captured an electron and $n_a(i) = 0$ if an acceptor is neutral. For the donors, $n_d(k) = 1$ if a donor on a donor site k is neutral and $n_d(k) = 0$ if a donor has given an electron away. We investigate the LES from the dielectric side of the MIT, so $\alpha_B < 1$ (α_B is the localization length of the electron on donor). The energy of the sample, assuming that all the interactions are of Coulomb origin, then is

$$E(n_a, n_d) = \frac{1}{2} \sum_{i \neq j} \frac{n_a(i) n_a(j)}{r_{ij}^{a-a}} + \frac{1}{2} \sum_{k \neq l} \frac{(1 - n_d(k)) (1 - n_d(l))}{r_{kl}^{d-d}} -$$

$$- \sum_{i,k} \frac{(1 - n_d(k)) n_a(i)}{r_{ik}^{a-d}} - \Delta \sum_i n_a(i), \quad (3)$$

where indices i, j and k, l number acceptor and donor sites, respectively, r_{ij}^{a-a} , r_{kl}^{d-d} and r_{ik}^{a-d} are the distances between the acceptors on the sites i and j , between the donors on the sites k and l , and between the acceptor on the site i and the donor on the site k , correspondingly, and Δ is the energy of charge transfer between acceptor and donors. When charge transfer occurs in the system, the energy of the sample changes by

$$\begin{aligned} \delta E(n_a, n_d) &= \sum_i \varepsilon_a(i) \delta n_a(i) + \sum_k \varepsilon_d(k) \delta n_d(k) + \\ &+ \sum_{i,k} \frac{\delta n_a(i) \delta n_d(k)}{r_{ik}^{a-d}} + \frac{1}{2} \sum_{i \neq j} \frac{\delta n_a(i) \delta n_a(j)}{r_{ij}^{a-a}} + \\ &+ \frac{1}{2} \sum_{k \neq l} \frac{\delta n_d(k) \delta n_d(l)}{r_{kl}^{d-d}}, \end{aligned} \quad (4)$$

where $\varepsilon_a(i)$ is the one-electron excitation (OEE) energy for the acceptors

$$\varepsilon_a(i) \equiv \frac{\delta E(n_a, n_d)}{\delta n_a(i)} = \sum_{j \neq i} \frac{n_a(j)}{r_{ij}^{a-a}} - \sum_k \frac{1 - n_d(k)}{r_{ik}^{a-d}} - \Delta, \quad (5)$$

$\varepsilon_d(i)$ is the corresponding OEE energy for the donors and $\delta n_a(i)$ ($\delta n_d(k)$) denotes the change of the occupation number on the acceptor (donor) site i (k). If a microscopic state (n_a^0, n_d^0) of the sample is the ground-state of this sample then for any excitation the relation

$$\delta E(n_a^0, n_d^0) \geq 0 \quad (6)$$

holds. The specific appearance of the conditions (6) depends on what excitations are allowed in the model system considered.

In the present paper we investigate the simplest case when only pairs of sites are involved in the charge transfer which, in turn, is allowed to occur in four different ways: (i) via electron hops between a pair of the acceptors $\{n_a(i) = 1, n_a(j) = 0\} \rightarrow \{n_a(i) = 0, n_a(j) = 1\}$; (ii) via electron hops between a pair of donors $\{n_d(k) = 1, n_d(l) = 0\} \rightarrow \{n_d(k) = 0, n_d(l) = 1\}$; (iii) via ionization process $\{n_a(i) = 0, n_d(k) = 1\} \rightarrow \{n_a(i) = 1, n_d(k) = 0\}$ and (iv) via recombination process $\{n_a(i) = 1, n_d(k) = 0\} \rightarrow \{n_a(i) = 0, n_d(k) = 1\}$. For each of those processes there is an unique set of $\{\delta n_a(i), \delta n_a(j), \delta n_d(k), \delta n_d(l)\}$. For instance, for the acceptor-acceptor hops

$$\delta n_a(i) = -1, \delta n_a(j) = 1, \delta n_d(k) = 0, \delta n_d(l) = 0. \quad (7)$$

Substituting (7) into (4) one obtains the ground-state stability relation with respect to the charge transfer between the pair of acceptors on the sites i and j

$$\varepsilon_a^0(j) - \varepsilon_a^1(i) - \frac{1}{r_{ij}^{a-a}} \geq 0, \quad (8)$$

where $\varepsilon_a^{1(0)}(i)$ denotes $\varepsilon_a(i)$ if $n(i) = 1(0)$. The stability conditions with respect to the other three manners of the charge transfer are obtainable in the similar manner.

The relation (8) implies that ε_a 's for the neutral acceptors are, in general, larger than ε_a 's for the charged acceptors. Furthermore, the pair of neutral and charged acceptors might be located on any distance and therefore in the thermodynamic limit the chemical potential for the acceptors (i. e. an energy level which separates the energies of the neutral and charged acceptors) is determined as

$$\mu_a = \min\{\varepsilon_a^0(i)\} = \max\{\varepsilon_a^1(i)\}. \quad (9)$$

Alike, there exist the chemical potential μ_d for the donors as well. Moreover, the stability relations with respect to the ionization and recombination lead to

$$\mu_a = \mu_d = \mu. \quad (10)$$

Despite the finite size of samples we investigated, the relation (10) with the chemical potentials calculated from (9) is valid within the limits of accuracy of our calculations (see Sect. III).

A macroscopic state of the sample \mathbf{R} is characterized by degree of acceptor ionization

$$C_a(\mathbf{R}) = \frac{1}{N} \sum_i n_a(i), \quad (11)$$

by the DOE for acceptors

$$g_a(\varepsilon_a, \mathbf{R}) = \frac{1}{N} \sum_i \delta(\varepsilon - \varepsilon_a(i)) \quad (12)$$

and by the corresponding DOE $g_d(\varepsilon_d, \mathbf{R})$ for the donors. Note, that for the finite samples (especially for the relative small systems we were able to investigate) $C_a(\mathbf{R})$, $g_a(\varepsilon_a, \mathbf{R})$ and $g_d(\varepsilon_d, \mathbf{R})$ depend essentially on the particular implementation \mathbf{R} of the spatial distributions of the donor and acceptor sites (if a sample would be big enough all quantities would be self-averaging). Therefore, in order to obtain reliable results, one has to work with the quantities $C_a \equiv \langle C_a(\mathbf{R}) \rangle$, $g_a(\varepsilon) \equiv \langle g_a(\varepsilon_a, \mathbf{R}) \rangle$ and $g_d(\varepsilon) \equiv \langle g_d(\varepsilon_d, \mathbf{R}) \rangle$, where $\langle \dots \rangle$ denotes the average over a number of \mathbf{R} 's. Note, that the values $g_{a(d)}(\varepsilon_{a(d)}, \mathbf{R}) d\varepsilon$ obtained for independent \mathbf{R} 's are scattered according to the Gaussian distribution with the mean $g_{a(d)}(\varepsilon) d\varepsilon$ and the standard deviation $\sqrt{g_{a(d)}(\varepsilon) d\varepsilon}$. In the region of the Coulomb gap $g_{a(d)}(\varepsilon) d\varepsilon \sim 10^{-4}$ and dispersion is several orders of magnitude larger than the mean. Therefore, in order to reduce the statistical noise in the final $g_{a(d)}(\varepsilon)$ dependences an average is needed over a sufficient large amount of independent samples (we performed calculations with up to 10^4 samples).

B. Acceptor-donor symmetry

Let us rewrite the energy (3) in terms of the OEE energies (5)

$$E(n_a, n_d) = \frac{1}{2} \sum_i \varepsilon_a(i) n_a(i) - \frac{1}{2} \sum_k \varepsilon_d(k) (1 - n_d(k)) - \frac{\Delta}{2} \sum_i n_a(i). \quad (13)$$

The system investigated is electrically neutral, i. e. for any sample

$$\sum_i n_a(i) = \sum_k (1 - n_d(k)). \quad (14)$$

Then, the energies of the microscopic states (n_a, n_d) and (n_a^*, n_d^*) for a sample \mathbf{R} and its “mirror” reflection \mathbf{R}^* (when the donor and acceptor sites exchange places keeping the spatial arrangement of sites unchanged), are equal under the following conditions

$$\varepsilon_a(i) + \varepsilon_d^*(i) = \varepsilon_d(k) + \varepsilon_a^*(k) = -\Delta \quad (15)$$

and

$$n_a^*(i) = (1 - n_d(i)) \quad n_d^*(k) = (1 - n_a(k)). \quad (16)$$

The stability relations (8) for the ground-state (n_a^0, n_d^0) of the sample \mathbf{R} transform into stability relations for the ground-state (n_a^{0*}, n_d^{0*}) of the sample \mathbf{R}^* through the relations (15,16) as well.

Since averaging over samples includes all possible pairs \mathbf{R} and \mathbf{R}^* , it follows from the symmetry relations (15) and (16) along with the definition (12) that $g_a(\varepsilon)$ can be mapped to $g_d(\varepsilon)$ using the relation

$$g_d(\varepsilon) = g_a(-\varepsilon - \Delta) \quad (17)$$

The symmetry of the model imposes also a relation between the Fermi energy μ (9,10) and the parameter Δ of the model. Expressing $n_{a[d]}(i[k])$ in terms of the Heaviside’s step functions $n_{a[d]} = \theta(\mu - \varepsilon_{a[d]}(i[k]))$, the quantity C_a can be written in the form

$$C_a = \int_{-\infty}^{\mu} g_a(\varepsilon) d\varepsilon = \int_{\mu}^{\infty} g_d(\varepsilon) d\varepsilon \quad (18)$$

The symmetry relation (17) transforms (18) into an integral relation

$$\int_{-\mu-\Delta}^{\infty} g_d(\varepsilon) d\varepsilon = \int_{\mu}^{\infty} g_d(\varepsilon) d\varepsilon, \quad (19)$$

which has a meaning only if

$$\mu = -\frac{\Delta}{2}. \quad (20)$$

Thus, the Fermi energy of our model system in the thermodynamic limit is a fundamental quantity depending only on the energy of charge transfer from an acceptor to a donor.

III. METHOD

A. Algorithm of energy minimization

We start from a random allocation of N donor and N acceptor sites in the continuous D -dimensional system (generate a sample \mathbf{R}) with the density $n = 1$, so that the system has a linear size $L = N^{1/D}$ and then charge randomly chosen $C_a \times N$ both donors and acceptors (usually we take $C_a = 0.7$), i. e. generate an initial microscopic state (IMS) (n_a, n_d) of the sample \mathbf{R} . Further, we search for such microscopic state (n_a^0, n_d^0) which obeys the stability conditions (8) with respect to the four mechanisms of the charge transfer allowed in our model. We used an algorithm which is an extension of the algorithm proposed in Ref. 9 to the case $\Delta \neq \infty$. The algorithm consists of the three main steps.

In order to save computer time, first, we look for pairs $a^0 - a^-$ ($d^0 - d^+$) for which the “crude” stability relation $\Delta\varepsilon \equiv \varepsilon_{a(d)}^0 - \varepsilon_{a(d)}^1 > 0$ is violated. Then, the energy of the system is decreased by transferring an electron between such pair of sites for which $\Delta\varepsilon$ has its minimal non-positive value. This process is repeated until a state is reached, in which $\Delta\varepsilon > 0$ for all possible $a^0 - a^-$ and $d^0 - d^+$ pairs (step I). In the similar manner, we further minimize the energy of the system with respect to the “true” stability relations (8) for the charge transfer between the $a^0 - a^-$ and $d^0 - d^+$ pairs (step II). And, finally, in the step III we diminish the energy of the system with respect to the stability relations for ionization and recombination processes. Since ionization and recombination processes change the degree C_a of the system ionization, each time after one of these processes takes place during calculations, we go back to the step II. Repeating the steps II and III, we finally arrive at a microscopic state (n_a^0, n_d^0) for which all four stability conditions are fulfilled. We name the procedure $(n_a, n_d) \rightarrow (n_a^0, n_d^0)$ via above steps I,II and III as “a single descent”.

It should be noted, however, that the state (n_a^0, n_d^0) is not necessarily the ground state of the sample \mathbf{R} since for the ground state, in general, not only the simplest relations (8) with only pairs of sites included, but the more complicated relations involving quadruplets, sextets, etc. of sites have to be fulfilled. Therefore, the state (n_a^0, n_d^0) (after Ref. 9) hereafter will be referred to as the pseudo-ground state (PGS) of the sample \mathbf{R} . Then, two questions naturally arise: How close the PGS and the ground state of the given sample are and how this may influence the output of our calculations? In order to answer the first question, we calculate and analyze the histograms \mathcal{H} for the so-called overlaps

$$Q_{\alpha\beta} = \frac{1}{N} \sum_i \delta(n_a^\alpha, n_a^\beta), \quad (21)$$

where indices α and β refer to PGS’s which are obtained by means of the single descent on the same sample but

with different IMS (n_a, n_d). If two PGS's are identical then $Q_{\alpha\beta} = 1$. We calculated for the $D = 2$ system with $N = 500$ at $\Delta = 0$ the mean $Q(\mathbf{R}) = \langle Q_{\alpha\beta} \rangle_{\alpha\beta}$ for the sequence of 100 PGS's generated by single descents from the different IMS of the same sample \mathbf{R} . We further acquire $Q(\mathbf{R})$ for 100 different samples and obtain that the mean $\bar{Q} \equiv \langle Q(\mathbf{R}) \rangle_{\mathbf{R}} = 0.96$. It means that in PGS generated by the single descent only 20 acceptors out of 500 are, in average, in the "wrong" states compared to those in the true ground state of the sample.

In order to evaluate how the "erroneousness" of PGS influences the outcome of our calculations we perform an analysis of ground states obtained by means of the so called multirank descents. Descent of rank m comprises of a consequence of the single descents on the same sample with different IMS when calculations are stopped after the lowest observed PGS energy repeats m times. We calculate \bar{Q} (all other parameters were the same as described in the previous paragraph, where actually the case $m = 0$ was explored) for descents with different ranks $m = 5, 10, 15$ and found that, for instance, for $m = 15$ (which implies drastic increase in the computation time) $\bar{Q} = 0.990$. $g_a(\varepsilon)$ and $g_d(\varepsilon)$ obtained from the PGS's generated by means of the single descents and by means of descents with $m = 10$, say, do not differ within the limits of statistical errors. So, we conclude, that reliable results can be obtained by means of single descents already, thereby saving a lot of computer time and resources.

B. Finite-size effects

Due to constraints in computer resources, the largest samples, we were able to deal with, comprise up to $N = 2000$ donor and $N = 2000$ acceptor sites ($L \sim 45$ for $D = 2$ and $L \sim 12$ for $D = 3$). Such relative small sizes of the samples investigated might influence the outcome of calculations. Detailed analysis of finite size effects on the results obtained will be presented in Section IV and here we want to make two remarks about inherent finite size effects in the model system considered.

First, as follows from (8), the energies ε_a^0 for the neutral acceptors and ε_a^1 for the charged ones in finite samples at $T = 0$ cannot be further away than $(L \times \sqrt{D})^{-1}$. This implies that $g(\varepsilon_a) = 0$ within the ε_a interval

$$|\varepsilon_a - \mu| < (2L \times \sqrt{D})^{-1} \quad (22)$$

Of course, the same holds for donors as well. The relation (22) gives the estimation how close to μ data on the energy spectrum are, in principle, obtainable from the calculations on finite samples.

Secondly, as follows from (5) the energies ε_a and ε_d for the finite samples are sensitive to the location of the donor and acceptor sites. Therefore, the Fermi energy μ for finite samples does differ, in general, from sample to

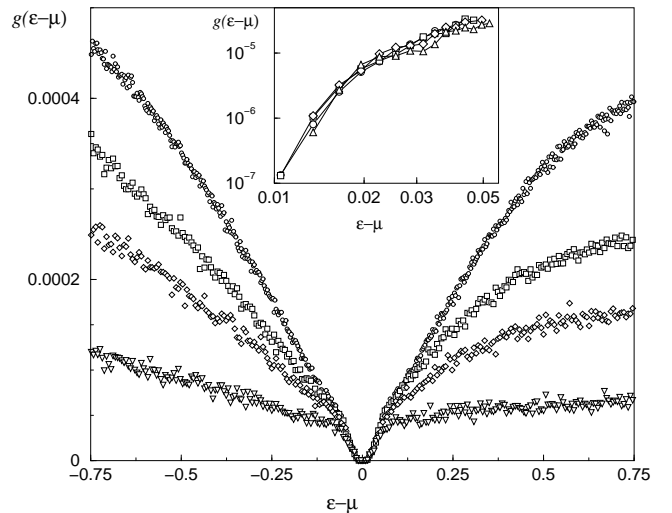


FIG. 1. Density of one electron excitations $g_a(\varepsilon - \mu)$ in the vicinity of the Fermi energy μ obtained for the two-dimensional model (3) with $N = 1500$ at $\Delta = 0$ (circles), 2 (squares), 4 (diamonds) and 10 (triangles). Data points presented in the figure are calculated as the average over 10.000 ($\Delta = 0$), 5.100 ($\Delta = 2$), 3.700 ($\Delta = 4$) and 2.200 ($\Delta = 10$) different samples. Insert shows double logarithmic plot of $g_a(\varepsilon - \mu)$ for $\varepsilon > \mu$ in the region $\varepsilon - \mu \lesssim 0.05$.

sample. A straightforward averaging of $g(\varepsilon)$ over different samples might thus lead to a distortion of the $g(\varepsilon)$ shape especially in the region where the Coulomb gap is observed. In order to avoid this undesired effect, we used a trick first proposed in Ref. 9. During accumulation of the results for $g(\varepsilon)$ we added together $g(\varepsilon)$ for the same values of $\varepsilon - \mu(\mathbf{R})$ rather than for the same values of ε . Here $\mu(\mathbf{R})$ denotes the Fermi energy for a finite sample \mathbf{R} calculated as

$$\mu(\mathbf{R}) = \frac{1}{2} \left(\min\{\varepsilon_a^0(i)\} + \max\{\varepsilon_a^1(i)\} \right), \quad (23)$$

Such way of doing $g(\varepsilon)$ average entirely excludes the influence of the fluctuations of the Fermi energy in the finite samples on the shape of the Coulomb gap.

Finally, we remark that all the data presented below were obtained for the open boundary condition. In order to ensure that results obtained are not determined by the type of the boundary conditions used in calculations, we performed calculations of the two-dimensional MCDAM at $\Delta = 0$ with different N and found that periodic boundary conditions only effectively reduce the linear size of a sample, leaving the qualitative shape of the parameters calculated unchanged.

IV. RESULTS

According to the symmetry relation (17) $g_a(\varepsilon)$ and $g_d(\varepsilon)$ can be easily mapped to each other for any values of ε and hence all the results presented below concern the acceptor sites only. One can expect that the

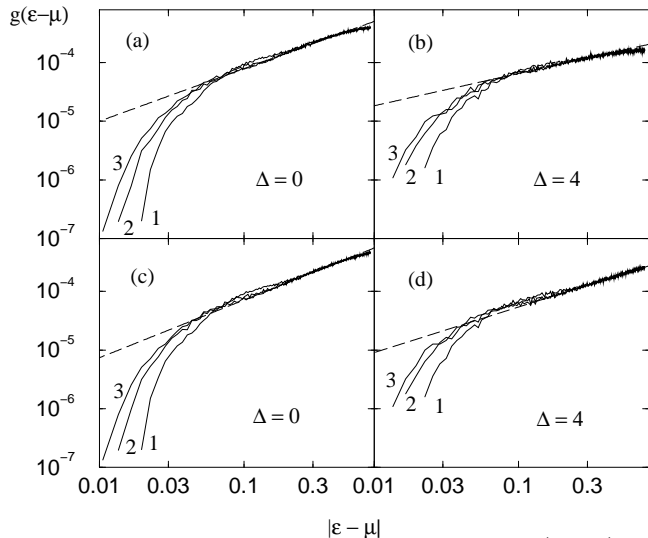


FIG. 2. Density of one electron excitations $g_a(\varepsilon - \mu)$ for $\varepsilon > \mu$ (a,b) and $\varepsilon < \mu$ (c,d) obtained for the two-dimensional model (3) at $\Delta = 0$ (a,c) and 4 (b,d), with $N = 500$ (curves numbered 1), 1000 (2) and 1500 (3). The dashed lines are least-squares power-law fits $g_a(\varepsilon - \mu) \sim |\varepsilon - \mu|^\gamma$ with $\gamma = 0.9$ (a), 0.55 (b), 0.98 (c) and 0.78. Data presented in the figure are calculated as the average over 10.000 different samples (except the case $N = 1500$ and $\Delta = 4$ with the average over 3700 different samples).

width of the Coulomb gap $\Delta\varepsilon$ and the energy scale in our model $E_0 = e^2 n^{1/D} / \chi$ are of the same order of magnitude. Fig.1 shows $g_a(\varepsilon - \mu)$ in the vicinity of the Fermi energy μ obtained for the two-dimensional samples with $N = 1000$ and various values of Δ . As it is seen, $g_a(\varepsilon - \mu)$ depends considerably on Δ except for a narrow window $|\varepsilon - \mu| \lesssim 0.05$, where all data merge into some “universal” curve symmetric with respect to μ , the curve which can be anticipated to obey the Efros universality hypothesis (1). However, a double-logarithmic plot of the “universal” $g_a(\varepsilon - \mu)$ (insert in the Fig.1), reveals that the behavior of $g_a(\varepsilon - \mu)$ in the “universality” region is not even a power law. The width of this “universality” region is comparable to the width of the region where $g_a(\varepsilon - \mu) = 0$ due to the finite size effects (for the data presented in Fig.1 relation (22) gives $|\varepsilon - \mu| < 0.011$), so it is plausible to suggest that the “universal” behavior of $g_a(\varepsilon - \mu)$ is governed by the finite-size effects. This is clearly demonstrated in Fig.2 where $g_a(\varepsilon - \mu)$ are shown for several sizes of the samples investigated.

The ε window where finite size effects are severe, shrinks considerably with increasing N for all values of Δ we investigated. For instance, $g_a(\varepsilon - \mu)$ for $N = 500$ and $N = 1000$ at $\Delta = 0$ (see Fig.2a,c) merge when $|\varepsilon - \mu| \gtrsim 0.2$ while corresponding curves for $N = 1000$ and $N = 1500$ are indistinguishable already at $|\varepsilon - \mu| \gtrsim 0.1$. The statistical noise observed for the curves in Fig.2 is quite small even close to μ and hence, the influence of insufficient large statistics on the results obtained is ex-

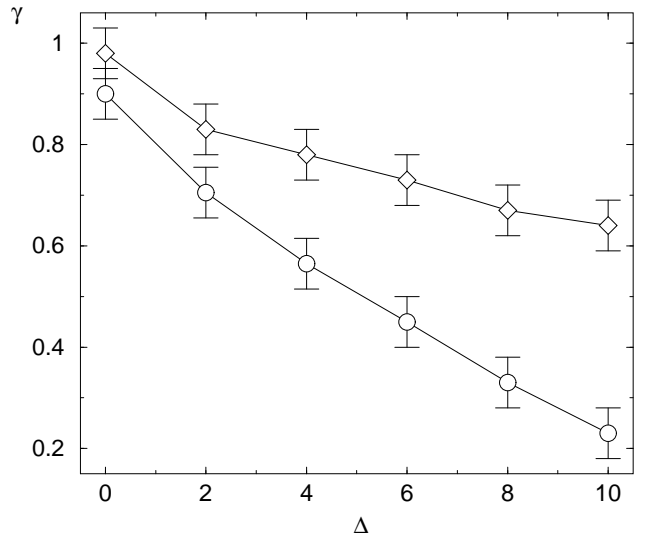


FIG. 3. The exponent γ of the power law $g_a(\varepsilon - \mu) \sim |\varepsilon - \mu|^\gamma$ as a function of the charge-transfer energy Δ . The data are obtained from least-squares fits of $g_a(\varepsilon - \mu)$ for the two-dimensional model (3) with $N = 1500$ within the region $0.2 \lesssim |\varepsilon - \mu| \lesssim 0.7$. Circles represent the positive values of $\varepsilon - \mu$ while diamonds stand for the negative values of $\varepsilon - \mu$. Lines are guides to the eye.

cluded. Note, that the “universal” behavior of $g(\varepsilon)$ in the vicinity of μ obtained for the classical $d - a$ model (see Fig.3 in Ref. 11) is most likely due to the finite size effects as well.

In the region $|\varepsilon - \mu| \gtrsim 0.2$, where the curves for all N collapse into a single curve (and where we believe the thermodynamic limit is reached), the behavior of $g_a(\varepsilon - \mu)$ is described by a power law $g_a(\varepsilon - \mu) \sim |\varepsilon - \mu|^\gamma$. The deviation from the power-law observed far away from μ ($|\varepsilon - \mu| \gtrsim 0.7$) is due to the boundaries of the Coulomb gap which, as was mentioned above, are ~ 1 in units of E_0 . One can see from a comparison of the data shown in Fig.2 for different Δ , that the exponent γ depends considerably on Δ . Furthermore, values of γ in the region $\varepsilon - \mu > 0$ and those in the region $\varepsilon - \mu < 0$ differ as well with this difference increasing with increasing Δ . The data for γ obtained for the two-dimensional MCDAM are summarized in Fig.3 where a significant deviation of γ from the value $D - 1$ predicted by the hypothesis (1) is observed at all values of Δ investigated except for the case $\Delta = 0$ when $\gamma \approx 1$ within the limits of statistical accuracy. Note, that the deviation of γ from its predicted value grows monotonically with increasing Δ . At $\Delta = 10$ where the features of the MCDAM are expected to be nearly the same as those of the classical $d - a$ model with all the acceptors being ionized (indeed, the degree of the acceptor ionization $C_a \sim 0.9$ for the two-dimensional MCDAM at $\Delta = 10$, see Fig.6 below) the deviation from the Efros exponent is very large.

The main results for $g_a(\varepsilon - \mu)$ obtained for the three-

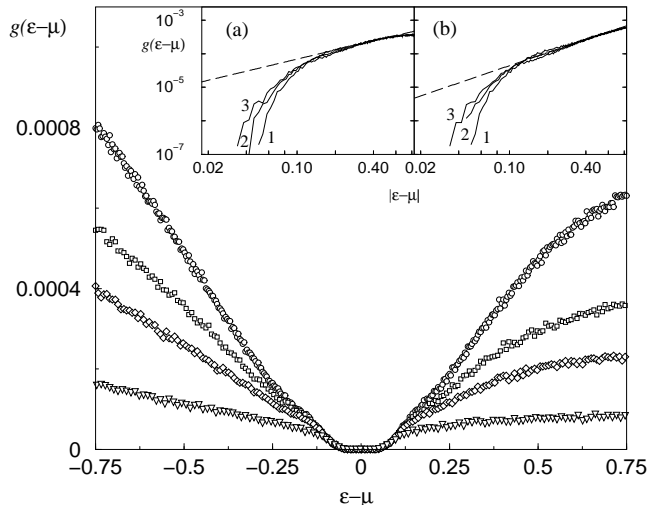


FIG. 4. Density of one electron excitations $g_a(\varepsilon - \mu)$ in the vicinity of the Fermi energy μ obtained for the three-dimensional model (3) with $N = 1000$ at $\Delta = 0$ (circles), 2 (squares), 4 (diamonds) and 10 (triangles). Data points presented in the figure are calculated as the average over 10.000 different samples. Inserts show double-logarithmic plots of $g_a(\varepsilon - \mu)$ at $\Delta = 2$, for $N = 500$ (curves numbered 1), 1000 (2) and 2000 (3), in the regions $\varepsilon > \mu$ (a) and for $\varepsilon < \mu$ (b). The dashed lines in the inserts are least-squares power-law fits $g_a(\varepsilon - \mu) \sim |\varepsilon - \mu|^\gamma$ with $\gamma = 1.16$ (a), 1.29 (b),

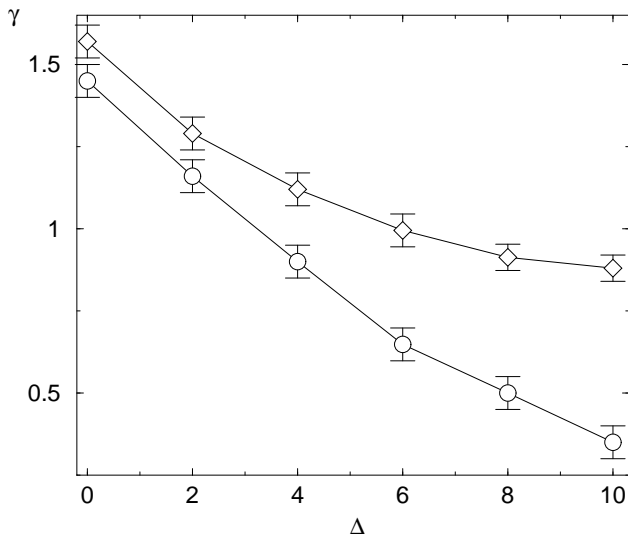


FIG. 5. The exponent γ of the power law $g_a(\varepsilon - \mu) \sim |\varepsilon - \mu|^\gamma$ as a function of the charge-transfer energy Δ . The data are obtained from least-squares fits of $g_a(\varepsilon - \mu)$ for the three-dimensional model (3) with $N = 1000$ within the region $0.4 \lesssim |\varepsilon - \mu| \lesssim 0.8$. Circles represent the positive values of $\varepsilon - \mu$ while diamonds stand for the negative values of $\varepsilon - \mu$. Lines are guides to the eye.

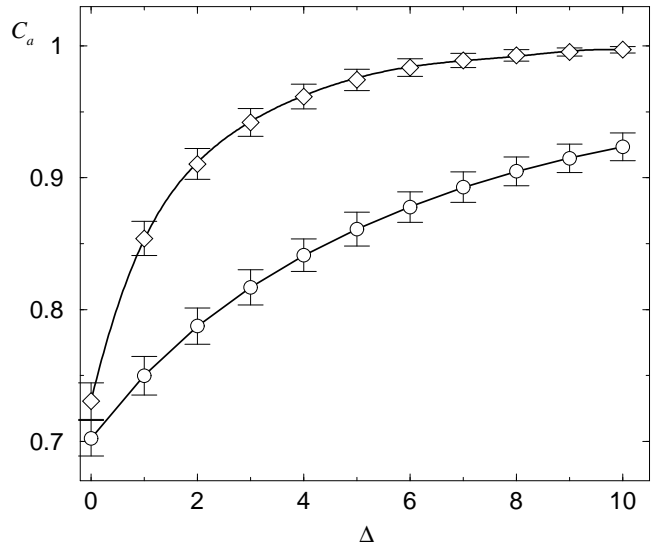


FIG. 6. The degree of acceptor ionization C_a as a function of the charge-transfer energy Δ . The data are obtained for the model (3) in two (circles) and three (diamonds) dimensions with $N = 500$ as an average over 1000 different samples. The solid lines are third-degree polynomial fits.

dimensional MCDAM are summarized in Figs. 4 and 5. It is seen, that the behavior of $g_a(\varepsilon - \mu)$ in three dimensions does not differ qualitatively from the behavior of $g_a(\varepsilon - \mu)$ in two dimensions. Some quantitative differences observed arise from the fact that at given N (the parameter which determines the amount of computer memory needed for the calculations) the linear size of a two-dimensional sample with a given density of sites is larger than that of a three-dimensional sample with the same density of sites and thereby, the finite size effects for three-dimensional samples with given N are more pronounced compared to those for the two-dimensional samples with the same N . For example, the lower boundary of the region where $g_a(\varepsilon - \mu)$ can be described by the power law $|\varepsilon - \mu|^\gamma$ shifts towards larger $|\varepsilon - \mu| \gtrsim 0.4$ values (see inserts in Fig.4). Remarkably, the exponent γ does not reach the value $D - 1$ predicted by the universality hypothesis (1) even at $\Delta = 0$ (Fig.5).

Unlike $g_a(\varepsilon - \mu)$ in the vicinity of the Coulomb gap, the density of ionized acceptors C_a (11) describes the state of the entire sample and therefore reaches the thermodynamic limit much faster than $g_a(\varepsilon - \mu)$. This allows us to obtain quite accurate results for C_a from data on a relatively small amount of samples with $N = 500$ only. Fig.6 shows the variations of C_a with Δ both for two and three dimensions. In three dimensions almost all acceptors become ionized ($C_a \sim 1$) rather soon while for two dimensions even for the largest Δ investigated around 10 % of the acceptors remain neutral. So, one can say, that the three-dimensional MCDAM at $\Delta \gtrsim 7$ reduces already to the classical $d - a$ model. It is known that the classical

TABLE I. The means $\bar{\mu}$ and standard deviations $\Delta\mu$ of the Fermi energy calculated for the three-dimensional model (3) with $N = 1000$ and various Δ .

Δ	$\bar{\mu}$	$\Delta\mu$
0	-0.017	0.100
2	-1.016	0.187
4	-2.0149	0.287
6	-3.016	0.392
8	-4.011	0.502
10	-5.018	0.607

$d - a$ model exhibits in three dimensions the, so called, Coulomb fluctuational catastrophe¹⁵. For calculations on finite samples it implies that statistical fluctuations of $\mu(\mathbf{R})$ grow dramatically with increasing Δ which is the case in our calculations (see Table I). Therefore, in order to reduce the statistical noise in three dimensions, the average of $g_a(\varepsilon - \mu)$ over a much larger (compared to $D = 2$) number of samples is needed. Note, that $\mu(\mathbf{R})$ in both two and three dimensions are scattered according to the Gaussian distribution with the mean $\bar{\mu}$ obeying the relation (20).

V. DISCUSSION

The behavior of $g_a(\varepsilon - \mu)$ calculated within the region of the Coulomb gap for the model (3) is in strong contradiction to the universality hypothesis (1). Despite the fact that $g_a(\varepsilon - \mu)$ is indeed described by the power law $|\varepsilon - \mu|^\gamma$ in a wide range of ε inside the region of the Coulomb gap, the exponent γ is considerably smaller than that predicted by the hypothesis (1) both for the two- and three-dimensional cases. Moreover, the exponent γ depends significantly on Δ and is different for the cases $\varepsilon > \mu$ and $\varepsilon < \mu$. It is believed that information about $g(\varepsilon)$ might be directly obtained from tunneling and photoemission experiments²² and recent experiments²³ on boron-doped silicon crystals have shown that the density of one-electron excitations at higher energies obeys a power-law with an exponent slightly less than 0.5 which is in good agreement with our results for $D = 3$ and $\Delta \gtrsim 8$. However, the non-metallic samples show around the Fermi energy a nearly quadratic Coulomb gap, so the question arises whether our results could be related to the intermediate asymptotic behavior observed? Here we want to make three remarks concerning this question:

First, the power law $g_a(\varepsilon - \mu) \sim |\varepsilon - \mu|^\gamma$ is valid above a value $\varepsilon_0(N)$ below which the finite size effects take over (Figs.2 and 4). It seems from our results, that $\varepsilon_0(N) \rightarrow \mu$ when $N \rightarrow \infty$. In two dimensions we were able to obtain size-independent results down to $\varepsilon_0 \sim 0.1$, i. e. for $\sim 90\%$ of the whole Coulomb gap, the halfwidth of which is ~ 1 in units of E_0 .

Secondly, as follows from the ground-state stability relations (2), the distance r_{ij} between a neutral donor, with an energy, say, $\varepsilon_i^1 \in [-\varepsilon, 0]$ (ε here is the halfwidth of a narrow band around $\mu = 0$) and a charged donor with an energy $\varepsilon_j^0 \in [0, \varepsilon]$ should be not less than $\frac{1}{2\varepsilon}$. I. e., sites with energies $\varepsilon_i^1 \in [-\varepsilon, 0]$ cannot be inside a D -dimensional sphere of radius $R_{sp} = \frac{1}{2\varepsilon}$ and with the center in a site with the energy $\varepsilon_j^0 \in [0, \varepsilon]$. Assuming that *all* such spheres *do not intersect*, the total volume occupied by the spheres is

$$V_{sp} = N \times S(D) \left(\frac{1}{2\varepsilon} \right)^D \int_0^\varepsilon g(\varepsilon') d\varepsilon' \quad (24)$$

where $S(D)$ is the volume of a D -dimensional sphere with the radius equal to unity. Since V_{sp} cannot exceed the total volume V of a sample ($V = N$ at $n = 1$) we arrive at the inequality

$$\int_0^\varepsilon g(\varepsilon') d\varepsilon' \leq \frac{(2\varepsilon)^D}{S(D)}, \quad (25)$$

which is valid for all ε if

$$g(\varepsilon) \leq \frac{D \times 2^D}{S(D)} |\varepsilon|^{D-1} \quad (26)$$

The universality hypothesis (1) then is a limit case of (26). The density of sites with energies $\varepsilon_i^1 \in [-\varepsilon, 0]$ indeed decreases when $\varepsilon \rightarrow 0$, so the assumption (24) for the spheres with *finite* radii seems to be plausible. However, simultaneously $R_{sp} \rightarrow \infty$ and consequently the plausibility of the assumption (24) and thereby of the hypothesis (1) becomes questionable.

And finally, the universality hypothesis (1) can be also obtained as the asymptotic behavior of a non-linear integral equation for $g(\varepsilon)$ as $\varepsilon \rightarrow 0$, the equation which, in turn, is heuristically obtained from the stability condition (2). The derivation of this integral equation (given, for example, in Ref. 17) is based on the implicit assumption that the sites with charged donors are randomly distributed in space according to the Poisson statistics. However, it was unequivocally demonstrated in computer studies of the Coulomb gap¹¹ that charged donor sites with energies close to μ tend to form clusters (Ref. 11, Fig. 6).

We conclude that $g_a(\varepsilon - \mu)$ in the region of the Coulomb gap in model (3) has a power law behavior for all energies down to μ and that the universality hypothesis of Efros (1) is questionable. Note, that our results are in contradiction not only to the universality hypothesis (1), but to the inequality (26) as well. Up to now, all exponents found are in good agreement with this inequality. E. g. in Ref. 12 specimens of 40 000 and 125 000 sites for two- and three-dimensional samples were investigated in the Efros' lattice model¹⁴ and the power law $g_a(\varepsilon - \mu) \sim |\varepsilon - \mu|^\gamma$ was found with $\gamma = 1.2 \pm 0.1$ and $\gamma = 2.6 \pm 0.2$ for two and three dimensions, respectively. The main conclusion

TABLE II. Some donor–acceptor pairs for which the difference between the donor and acceptor energy levels does not exceed 10 meV. E_g , E_v and E_c are, respectively, the energy gap, the top of the valence band and the bottom of the conductivity band. If the solubilities of both donor and acceptor are known, the parameter E_0 is calculated using the data for the less soluble of the pair.

Donor	Acceptor	Solubility, cm^{-3}		E_0 , meV		E_j , meV	Δ , meV
		min	max	min	max		
Si ($E_g = 1124$ meV, $\chi = 12$)							
Fe	Zn	1.2×10^{16}	4×10^{16}	0.6	4	$E_c - 796$	8
		2.3×10^{16}	8×10^{16}			$E_v + 320$	
Ni	In	10^{18}	10^{13}	12	< 1	$E_v + (160 \div 190)$	3.1 – 33.1
		3×10^{17}	4×10^{18}			$E_v + 156.9$	
Ge ($E_g = 740$ meV, $\chi = 15.9$)							
S	Ni	no reliable data		1.5	1.8	$E_c - 296$	4
		4.8×10^{15}	8×10^{15}			$E_c - 300$	
GaAs ($E_g = 1520$ meV, $\chi = 12.5$)							
Ti	Fe	2×10^{16}	-	3.1	-	$E_c - 1000$	0
						$E_v + 520$	

of our results and those of Ref. 12 is that Efros’ lattice model¹⁴ can not be used to as a reliable approximation to the classical $d - a$ model with Poisson impurity distribution. Energy levels of donor (acceptor) impurities are usually close to the bottom (top) of the conduction (valence) band. Since in the most common semiconductors the energy gap $E_g \sim 10^4$ K and $E_0 \sim 20$ K, $\Delta \gg 1$ and one may ask what physical relevance does the model (3) with a finite $\Delta \lesssim 10$ have, except for being a pure academic exercise? However, in the case of deep impurities the energy levels for some donor–acceptor pairs are extremely close to each other not excluding even the case $\Delta = 0$ ²⁴. Table II shows some donor–acceptor pairs with $\Delta \lesssim 10$ in the most common semiconductors. The solubilities of these impurities are rather low, thereby reducing the temperature at which the Coulomb gap with features described by the model (3) can be observed. Fortunately, these temperatures are high enough ($\sim 10 \div 20$ K) for modern experimental techniques and hence experimental observation of the Coulomb gap in the semiconductors with deep impurities is possible to accomplish.

VI. SUMMARY

We have studied a model of impurities in semiconductors with infinite-range Coulomb interactions between donors, between acceptors and between donors and acceptors. A new parameter introduced in the model is the finite energy Δ of charge transfer between donors and acceptors, a parameter which enables processes of ionization of neutral impurities and of recombination

of charged impurities. In the particular case of equal amounts of donor and acceptor impurities, we derived rigorous relations for the symmetry of the model with respect to exchange of donor and acceptor sites. We also extended the previously known algorithm to find the ground state including the stability relations with respect to ionization and recombination processes and performed computer studies of the model proposed at zero temperature on a number of two- and three-dimensional samples with randomly distributed N donors and N acceptors. We explored the energy region around the Fermi energy μ where the Coulomb gap in the density of one-electron excitations $g(\varepsilon)$ is observed. The analysis of the calculated histograms $g(\varepsilon)$ revealed that the behavior of $g(\varepsilon)$ obtained from the simulations on finite samples in the immediate neighborhood of μ is determined solely by the finite size effects. In the region where finite size effects become negligible $g(\varepsilon)$ is described by a power law with an exponent considerably depending on the parameter Δ and on the sign of $\varepsilon - \mu$. Our findings challenge the Efros universality hypothesis. Moreover, our results are in contradiction to the main inequality (26) of which Efros’ universality hypothesis is a particular case. We have reexamined the heuristic derivation of the Efros hypothesis and shown that some implicit assumptions which lead to universality are questionable. From the analysis of experimental data on admixtures in semiconductors we put forward possible experimental situations where one could observe the Coulomb gap with the features being the same as those of the model with a finite Δ .

ACKNOWLEDGEMENTS

This research was supported by The Swedish Natural Science Council and by The Swedish Royal Academy of Sciences.

-
- ¹ M. Pollak, *Discuss. Faraday Soc.* **50**, 13 (1970); G. Srinivasan, *Phys. Rev. B* **4**, 2581 (1971); V. Ambegaokar, B. J. Halperin and J. S. Langer, *Phys. Rev. B* **4**, 2612 (1971).
- ² B. L. Altshuler and A. G. Aronov, *Solid State Comm.* **30**, 115 (1979).
- ³ W. L. McMillan and J. Mochel, *Phys. Rev. Lett.* **46**, 556 (1981); G. Hertel, D. J. Bishop, E. G. Spencer, J. M. Rowell and R. C. Dynes, *Phys. Rev. Lett.* **50**, 743 (1983).
- ⁴ J. Imry and Ovadyahu, *Phys. Rev. Lett.* **49**, 841 (1982); A. E. White, R. C. Dynes and J. P. Garno, *Phys. Rev. B* **31**, 1174 (1985).
- ⁵ N. F. Mott, *J. Non-Cryst. Solids* **1**, 1 (1968).
- ⁶ A. L. Efros and B. I. Shklovskii, *J. Phys.* **C8**, L49 (1975); B. I. Shklovskii and A. L. Efros, *Sov. Phys. Semicond.* **14**, 487 (1980).
- ⁷ M. A. Pollak, *J. Non-Cryst. Solids* **11**, 1 (1972); E. M. Hamilton, *Philos. Mag.* **26**, 1043 (1972).
- ⁸ S. D. Baranovskii, B. I. Shklovskii and A. L. Efros, *Sov. Phys. – JETP* **51**, 199 (1980).
- ⁹ S. D. Baranovskii, A. L. Efros, B. I. Gelmont, and B. I. Shklovskii, *J. Phys.* **C12**, 1023 (1979).
- ¹⁰ A. L. Efros, N. van Lien and B. I. Shklovskii, *J. Phys.* **C12**, 1869 (1979); S. D. Baranovskii, A. A. Usakov and A. L. Efros, *Sov. Phys. – JETP* **56**, 422 (1982).
- ¹¹ J. H. Davies, P. A. Lee and T. M. Rice, *Phys. Rev. B* **29**, 4260 (1984).
- ¹² A. Möbius and M. R. Richter, *J. Phys.* **C20**, 539 (1988); A. Möbius, M. R. Richter and B. Drittler, *Phys. Rev. B* **45**, 11568 (1992).
- ¹³ K. Tenelsen and M. Schreiber, *Europhys. Lett.* **21**, 697 (1993); *Phys. Rev. B* **49**, 12 662 (1994).
- ¹⁴ A. L. Efros, *J. Phys.* **C9**, 2021 (1976).
- ¹⁵ B. I. Shklovskii and A. L. Efros “*Electronic Properties of Doped Semiconductors*” (Springer-Verlag, Berlin 1984).
- ¹⁶ A. L. Burin, *J. Low Temp. Phys.* **100**, 309 (1995).
- ¹⁷ A. A. Mogilyansky and M. E. Raich, *Sov. Phys. JETP* **68**, 1081 (1989).
- ¹⁸ E. R. Grannan and C. C. Yu, *Phys. Rev. Lett.* **71**, 3335 (1993).
- ¹⁹ V. N. Likhachev and V. A. Onishchouk, *Phys. Lett.* **A244**, 437 (1998).
- ²⁰ T. Vojta and M. Schreiber, *Phys. Rev. Lett.* **73**, 2933 (1994).
- ²¹ M. Mezard, G. Parisi and M. A. Virasoro “*Spin Glasses Theory and Beyond*”, World Scientific, Singapore, 1987.
- ²² A. E. White, R. C. Dynes and J. P. Garno, *Phys. Rev. Lett.* **56**, 532 (1986); J. G. Massey and M. Lee, *Phys. Rev. Lett.* **75**, 4266 (1995).
- ²³ M. Lee, J. G. Massey, V. L. Nguyen, and B. I. Shklovskii, *Phys. Rev. B* **60**, 1582 (1999).
- ²⁴ *Semiconductors: Impurities and Defects in Group IV Elements and III-V Compounds*, Landolt-Börnstein New Series, v. III/22, Ed. M. Schulz, Springer-Verlag, Berlin, 1989; A. Bargys and J. Kundrotas “*Handbook on physical properties of Ge, Si, GaAs and InP*”, Science and Encyclopedia Publ., Vilnius, 1994.